Underlay Interference Analysis of Power Control and Receiver Association Schemes

Sachitha Kusaladharma, Prasanna Herath, *Student Member, IEEE*, and Chintha Tellambura, *Fellow, IEEE*

***Abstract*—In this paper, we present a precise, comprehensive analysis of the aggregate interference (I) generated from an underlay network of cognitive radio (CR) nodes employing several transmit power control and receiver association schemes. Importantly, we consider spatial randomness by modeling CR transmitter nodes and receiver nodes as two independent Poisson Point Processes. For the cognitive nodes, we investigate receiver association based on the distance or the instantaneous received power and power control based on the maximum possible transmitter-receiver distance, fixed or location dependent cut-off power levels, feedback from the primary system, or the maximum number of available receivers. For each of these schemes, the exact moment generating function (MGF) and mean of aggregate I power are derived for links with Rayleigh fading and exponential path loss. The resulting primary outage and the probability of secondary transmitter cut-off are also derived. Numerical results show that the secondary power thresholds and node densities significantly affect the aggregate I, primary receiver outage, and secondary transmitter cut-off arising from the different schemes.**

***Index Terms*—Interference analysis, underlay networks, stochastic geometry, point process theory, power control**

I. Introduction

Since spectrum scarcity and under utilization are two factors inhibiting the growth of wireless networks, more dynamic, agile ways to utilize wireless spectrum are necessary [2]. Thus, in cognitive radio (CR), a node can automatically detect which spectrum slots are in use by licensed (primary) users and which are not, and it can opportunistically transmit over vacant channels. This mode of operation clearly optimizes the spectrum usage while minimizing interference to licensed users [2]. Such nodes are referred to as cognitive or secondary nodes. The standardization of cognitive networks has already begun with IEEE 802.22 (television white spaces), ECMA 392, IEEE 802.11af, and DySPAN 1900.7 coming into the fray [3]. Cognitive concepts may also feature in the development of fifth generation of cellular networks [4].

In practice, cognitive or secondary nodes may operate in underlay, overlay, or interweave mode [2]. The underlay mode is especially attractive because both primary and cognitive nodes transmit simultaneously over a given spectrum slot, thereby achieving high spectral efficiency [2], [5], [6]. It can also be used in device to device (D2D) networks, cognitive femtocells, sensor networks, personal area networks, and small cell networks. However, because of the imposition of interference power (I) constraints for the primary user's protection, underlay nodes must use transmit power control, which is the main limiting factor of their capacity. Nevertheless, each underlay node can still achieve half of the total degrees of freedom which would have been attainable without interference constraints [2].

Thus, transmit power control, contention control, and receiver association schemes must be used not only to manage interference at the primary network, but also to improve the throughput, reliability and other quality-of-service parameters associated with the underlay network itself. While these schemes are widely used in wireless systems, their use in underlay networks has not been investigated extensively.

1) Power control methods have been widely used in non-cognitive set-ups to reduce the signal to interference ratio. Those include fixed power, distance based schemes with channel inversion, and measurement based schemes [7]. For example, open-loop and closed-loop schemes are used in Wideband Code Division Multiple Access (WCDMA) and Long Term Evolution (LTE) networks [8]. Although such schemes have been extensively studied for non-cognitive settings [9]–[12], how they perform in terms of minimizing the interference from cognitive underlay networks remains to be quantified.
2) Contention control can also help to reduce interference. which limits the transmissions of a node based on its distance to other nodes [13]. These can be employed together with or independently from power control schemes, and have been shown to significantly reduce the mean I [13].
3) Receiver association schemes specify which receiver is selected by a transmitter. They can be based on the distance, the instantaneous signal to noise ratios (SNRs), or the received powers of pilot signals of the transmitter-receiver channels [14]. For example, the transmitter can be associated with the nearest receiver, or the receiver with the highest received power.

While the aforementioned schemes do help to reduce I from cognitive nodes, additional reduction of I is possible via two other mechanisms: namely, instituting cut-off transmit powers for cognitive transmitters and enforcing exclusion regions around the primary nodes. The cut-off transmit power, which is the maximum transmit power level allowed for cognitive transmitters can either be a constant or location dependent. An exclusion (guard) region around the primary nodes defines a region where cognitive nodes are barred from transmitting. These can be enforced either through prior location informa-

This work, in part, was presented at the IEEE International Conference on Communications (ICC), Sydney, Australia, June 2014 [1].

S. Kusaladharma, P. Herath, and C. Tellambura are with the Department of Electrical and Computer Engineering, University of Alberta, Edmonton, AB, Canada T6G 1H9 (e-mail: kusaladh@ualberta.ca, prasanna@ualberta.ca chintha@ece.ualberta.ca). P. Herath is also with the Telecommunications Research Laboratories, Edmonton, Canada, T5K 2M5.

tion which could be obtained through a centralized control center aided by GPS data, or dynamically via sensing pilot signals/acknowledgements originating from the primary nodes [6], [13], [15].

A. Prior research

Aggregate I of random cognitive networks has been extensively analyzed including statistical interference models, exact analysis, and performance bounds [15]–[29]. For example, [15] provides a statistical model for I considering path loss, small scale fading, shadowing, sensing techniques, and also investigates the effects of primary network transmit power control. Interference in a spectrum sensing framework [16] and heterogeneous networks (networks with multiple tiers of nodes) with macro base stations and cognitive femto access points [17] have been analyzed. On the other hand, [19] derives the moment generating function (MGF) and cumulants of I. Centralized and distributed power control schemes for a D2D network are proposed in [20]. A normal and log-normal sum approximation is developed in [21], while [22] approximates the interference with the nearest neighbor's interference. The average I considering intra-cognitive user interference has been derived in [23], while a coverage analysis of two tier networks is performed in [24]. The MGF of the underlay I is analyzed and approximated in [25] while considering the effects of shadowing. Moreover, [26] investigates the effects of the exclusion zone radius and the number of cognitive nodes whereas [27] analyses the probability density function (PDF) of the interference under different exclusion regions. Reference [28] analyzes I due to beacon misdetection for hybrid underlay-interweave networks, while [30] develops a foundation for designing wireless networks with secrecy exploiting intrinsic spatial and channel properties of the wireless environment. Bounds for interference and outage probability are derived and a method involving Poisson cluster processes to model the interference is proposed in [29] for active cognitive nodes outside primary node guard regions following a Poisson hole process, while power control strategies based on single node optimal power control and the Nash equilibrium for interference limited Poisson distributed nodes are studied in [31]. Furthermore, [32] proposes a technique to estimate access point throughput in dense random CSMA (Carrier Sense Multiple Access) networks, and extends the results when the access points form a Matern-hardcore process using an computationally efficient procedure.

B. Motivation

Thus, prior research has not completely analyzed the impact of power control, receiver association, and contention control schemes on I (interference on primary network) and on the performance of the cognitive network itself. Publications [19], [23], [26] have assumed a constant transmit power for cognitive nodes, and in the case of [32] for the transmitting access points. Whilst enabling analytical tractability, this assumption may not hold because the actual transmit powers depend on several factors including the receiver association policy, the distance to the intended receiver, and the cut-off transmit power. Thus, all such factors must be considered in a more comprehensive analysis. While a channel inversion based power controlling scheme and a threshold scheduling scheme are proposed in [33] for an infinite network, [33] does not consider different receiver association models and guard regions. Furthermore, cut-off thresholds or maximum allowable receiver distances are not considered for the power control schemes. A comprehensive analysis is given by [13], which provides a rigorous analysis of power control, contention control, and hybrid power-contention control schemes by deriving the primary receiver interference in an underlay network with exclusion regions. The power control technique adopted in [13] limits the mutual interference among cognitive transmitters but only considers one spatial point process for cognitive nodes. No distinction is thus made between a transmitter node and receiver node. In contrast, we differentiate cognitive transmitters and receivers by modeling them as two separate spatial point processes, which allows for more detailed analysis of the system. Our approach also focuses on guaranteeing a certain level of performance for the cognitive receivers. Therefore, our work complements [13] and develops several interference management schemes. These schemes thus enable various trade-offs among performance objectives, thereby offering a more flexible system analysis and design perspective. Finally, the primary objective of this paper is to provide an exact analysis of the aggregate I for the proposed association and power control policies in underlay networks.

C. Contributions

We propose several interference management schemes for the cognitive nodes, derive the MGF and mean aggregate I and analyze the outage of the primary receiver. The proposed schemes are as follows:

- Nearest receiver association with power control schemes based on: 1) cognitive transmitter-receiver distance r_c 2) r_c and a constant cut-off power level 3) r_c and a location dependent cut-off power level.
- Nearest-M receiver association with the power control scheme based on the transmitter receiver distance $r_{c,k}$ and a constant cut-off power level.
- Best received power association (when channel state information (CSI) is available) with the following: 1) power control based on the transmitter receiver distance, the channel state information, and a constant cut-off power level 2) constant powered transmission with self deactivation based on the estimated received power at the receiver.
- Nearest-M receiver association and transmission restrictions based on distance to other receivers.
- Iterative changing of the cut-off transmit power level based on the primary receiver performance with a nearest receiver association, a power control scheme based on the transmitter receiver distance and, a cut-off power level.

The MGF is an extremely important tool for deriving various statistics. For instance, while immediately providing moments, which can be used moment matching purposes, it can also be used for evaluations bit error rates and outage [34], [35].

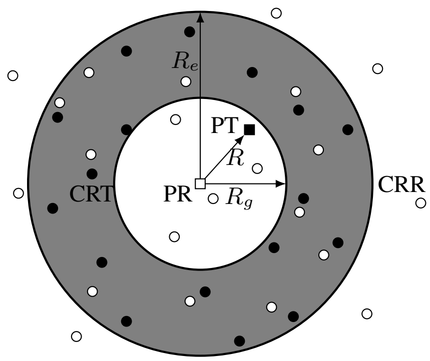

Fig. 1: Sytem model. The PR is located at (0,0). Active cognitive transmitters are in the shaded area. Respectively, R_g, R_e, R, PT, CRT, and CRR denote the guard distance, the outer distance, the primary transmitter-receiver distance, the primary transmitter, a cognitive transmitter node, and a cognitive receiver node.

Furthermore, the probability of a cognitive transmitter being cut-off is derived. Moreover, for the best received power association, we will use stochastic-geometry tools including the Mapping and Marking theorems [36] to derive the distance distribution to a cognitive receiver having the best received power.

The following system-model assumptions are made: 1) the cognitive transmitter and receiver nodes form two independent homogeneous Poisson point processes (PPPs) [36] 2) the exclusion zone around the primary receiver Fig. 1 is perfectly enforced 3) The links experience exponential path-loss and Rayleigh fading 4) CSI may or may not be available 5) cognitive transmitters know the distances to cognitive receivers (either via pilot signals, or through information stored in a database).

This paper is organized as follows. Section II introduces the spatial and signal models. Section III derives the MGF and mean of the aggregate I for the proposed transmission schemes, while Section IV derives the outage probability of the PR. Section V provides numerical results, and Section VI concludes the paper.

Notations: $\Gamma(x,a)=\int_a^\infty t^{x-1}e^{-t}dt$, $\Gamma(x)=\Gamma(x,0)$, and ${}_2F_1(,;,)$ is the Gauss Hypergeometric function [37]. $\Pr[A]$ is the probability of event A, $f_X(\cdot)$ is the PDF, $F_X(\cdot)$ is the cumulative distribution function (CDF), $M_X(\cdot)$ is the MGF, and $E_X[\cdot]$ denotes the expectation over random variable X. Bernoulli(p) is a random variable X with $\Pr[X=1]=p$ and $\Pr[X=0]=1-p$. For $x\in\mathbb{R}^2$, $||x||$ is the Euclidean norm.

II. System model

This section introduces both the spatial and signal models.

A. Spatial model and assumptions

- Without loss of generality, the PR is located at the center with a distance R from the primary transmitter.
- The active cognitive transmitters are located in a finite annular area (Fig. 1). The circle of radius R_g around the PR is the exclusion zone, which plays an important role to limit the interference [19]. The value of R_g will be decided based on the maximum admissible outage probability for a primary receiver. The cognitive transmitters within the exclusion zone do not transmit or must use a different frequency block. We further assume that the cognitive transmitters lie within a finite outer radius of R_e in order to provide a more general analysis (the secondary network may form a single cluster where a finite R_e may be the most appropriate). Note that a field of active cognitive transmitters distributed in the entire $\mathbb{R}^2$ is a special case of our model when $R_g\to 0$ and $R_e\to\infty$. The cognitive receivers are distributed in $\mathbb{R}^2$.
- Because the number and locations of cognitive transmitters and receivers are random, they must be modeled by a spatial stochastic process [18], [38], [39]. For this purpose, independent homogeneous PPPs with intensities λ_t and λ_r respectively are used. We will denote them as Φ_t and Φ_r respectively. Thus Φ_t or Φ_r is a point processes in $\mathbb{R}^2$ with uniform intensity $\lambda>0$ ($\lambda\in\{\lambda_t,\lambda_r\}$) such that: (a) for every bounded closed set A, the number $N(A)$ is Poisson distributed with
$$\Pr[N(A)=n]=\frac{(\lambda A)^n}{n!}e^{-\lambda A}, n=0,1,2,\dots \tag{1}$$
and (b) if $A_1,A_2\dots,A_m$ are disjoint sets, $N(A_1),N(A_2),\dots,N(A_m)$ are independent random variables [40]. The PPP has extensively been used to characterize the spatial distribution of cognitive radio nodes in prior research [13], [15], [19].

Let $\phi_{t,i}$ denote the i-th cognitive transmitter located at $x_i\in\Phi_t$ when it exists. Thus, the distance to the PR from $\phi_{t,i}$ r_i is $r_i=||x_i||$, $R_g<r_i<R_e$. The distribution of r_i is obtained as follows. Because Φ_t is a homogeneous PPP, the CDF of r_i becomes $F_{r_i}(x)=\frac{\pi(x^2-R_g^2)}{A_t}$, $R_g<x<R_e$, where $A_t=\pi\left(R_e^2-R_g^2\right)$. Differentiating this CDF yields the PDF [25]
$$f_{r_i}(x)=\begin{cases}2\frac{\pi x}{A_t} & , R_g<x<R_e\\ 0 & , \text{otherwise}\end{cases}. \tag{2}$$

Let $\phi_{r,k\backslash i}$ denote the k-th closest receiver from $\phi_{t,i}$ located at $y_{k\backslash i}\in\Phi_r$. We will require the distribution of the distance to $\phi_{r,k\backslash i}$ from $\phi_{t,i}$, which we will denote as $r_{c,k}$ where $r_{c,k}=||y_{k\backslash i}-x_i||$. Because Φ_r and Φ_t are stationary, $r_{c,k}$ is equivalent to the distance to the k-th nearest node in a PPP from any given location. The CDF of $r_{c,k}$ can be obtained by considering the probability of having at least k nodes within a circle of radius x;
$$F_{r_{c,k}}(x)=1-\sum_{i=0}^{k-1}\frac{(\lambda_r\pi x^2)^i}{i!}e^{-\lambda_r\pi x^2}, 0<x<\infty.$$
Thus, the PDF of $r_{c,k}$ is thus obtained as [41], [42]
$$f_{r_{c,k}}(x)=\frac{2(\pi\lambda_r)^k}{(k-1)!}x^{2k-1}e^{-\pi\lambda_r x^2}, 0<x<\infty. \tag{3}$$
When $k=1$, we get the distance distribution to the nearest receiver node from $\phi_{t,i}$ ($r_{c,1}$). We will refer this distance as r_c for brevity.

In the subsequent analysis, we assume that all $\phi_{t,i}$ in the annular region with $R_g<||x_i||<R_e$ are active simultaneously. However, this is a worst-case assumption designed to

glean maximum primary interference level. Nevertheless, there is no loss of generality in this assumption because if some transmitters are inactive, we can model this on-off behaviour by assigning a transmission probability $\beta < 1$ to each node. By using independent thinning [36], our derived expressions can then be adapted by replacing λ_t with $\beta\lambda_t$.

We will investigate nearest receiver association, the best received power association, and k-th nearest receiver association. Practical applications for such networks can include ad-hoc networks, wireless sensor networks, and cellular networks [43].

B. Signal model

- All radio links experience path-loss, and the power law path loss model (log-distance path loss model) [44] is assumed. Accordingly, the received power at a distance r from the transmitter may be expressed as $P_r = Pr^{-\alpha}$, where α is the path-loss exponent, and the constant $P = P_0 r_0^{\alpha}$ is termed the power level. The path-loss exponent varies between 1.6 (same floor in office buildings) to 6.5 (built up areas) [44]. To complete this model, P_0 is the received power at a reference distance of r_0. Typically, r_0 varies from 1 m (pico cells) to 1 km (macro cells). For a given r_0, the received power P_0 depends on the frequency, antenna heights, buildings and other factors.
- Small-scale fading is modeled by the Rayleigh model, for which the PDF of the i-th channel power gain is Exponential and is given by $f_{|h_i|^2}(x) = e^{-x}, 0 \leq x < \infty$.

The interference from $\phi_{t,i}$, I_i can thus be written as [19]

$$I_i = P_i |h_i|^2 r_i^{-\alpha}, \tag{4}$$

where r_i and P_i are respectively the distance from the PR and the power of $\phi_{t,i}$. The aggregate interference I is [19]

$$I = \sum_{i=1}^{N} I_i, \tag{5}$$

where N is the number of cognitive transmitters.

C. Power control and association model

The following receiver association schemes are considered in this paper for cognitive nodes:

- **Nearest association**: a transmitter thus is connected with its nearest receiver (denoted as $\phi_{r,1\setminus i}$). The benefits are: (1) instantaneous channel state information (CSI) is not required, (2) the highest received power averaged over small scale fading is achieved, and (3) the distance to the nearest receiver may be found readily.
- **Nearest-M association**: a transmitter thus selects a neighbor within its M closest neighbors. Of course, $M = 1$ is the above case. The transmitter successively checks the availability of a receiver, starting from the closest node to the farthest one in the set.
- **Best received power association**: a transmitter is associated with the receiver having the highest received power. We will denote this receiver as $\phi_{r,p\setminus i}$. The receiver thus may or may not be the nearest. Such schemes require the use of periodic pilot/beacon signals from the receivers to obtain CSI [45]. These schemes are thus more complex than the nearest association schemes.

For each of the above association techniques, we assume that a receiver may be associated with more than one transmitter at a given time[1]. Moreover, although there will be certain correlations in the transmit power of different transmitters, the impact of ignoring such correlations is minor as shown in simulations of Section V.

For each of the above schemes, we consider several power control methods at the transmitter. All the power control schemes can be summed up by the following equation for the transmit power (P_i):

$$P_i = \begin{cases} P_s r^{\alpha} (|h|^2)^{\mu} & , P_s r^{\alpha} (|h|^2)^{\mu} < P_c \\ 0 & , \text{otherwise} \end{cases}. \tag{6}$$

In this equation, $|h|^2$ and r are the channel gain due to small scale fading and distance between the cognitive transmitter and the associated receiver, P_s is the required average received power at the cognitive receiver, P_c is the cut-off power level, and $\mu \in \{0, -1\}$.

The individual power control methods are as follows:

- Path loss inversion: this negates the attenuation due to path loss and ensures a constant received power regardless of the distance. Distance information between the transmitter and the associated receiver is needed for this to be effective. ($\mu = 0$, $P_c = \infty$)
- Channel inversion: With channel inversion, the whole channel gain (path loss and small scale fading) is inverted. However, CSI of the transmitter-receiver channel is essential.
- Constant cut-off power level: $P_i < P_c$ where P_c is constant and finite.
- Location dependent cut-off power level: The premise of this is similar to a constant cut-off power level except for the fact that the cut-off power level varies by location. The interference from a cognitive node on the PR depends greatly on its distance from the PR. Thus, a constant cut-off power threshold disadvantages cognitive nodes which are far away. In this scheme, the cut-off power level may vary with its distance to the PR.
- Iteratively changing cut-off power: Feedback information from the primary system is used to iteratively change the cut-off power level to balance PR outage and cognitive transmitter cut-off probability.
- Constant powered transmission with self deactivation: Each transmitter employs a constant power to transmit. Before a transmission occurs, the transmitter estimates the received power level at the associated receiver, and if this falls below the required threshold, the transmission is aborted. This method also requires CSI.

Moreover, we also investigate transmission restrictions based on distances to other cognitive receivers where, a cognitive transmitter will refrain from transmitting if desired

[1]The secondary network may employ multiple access techniques within the given frequency block, but a detailed discussion is out of the scope of this paper.

cognitive receivers do not exist within an association region. The existence of cognitive receivers within the association region can be found out using GPS information disseminated through a centralized control center.

Transmission restrictions may also be enforced based on distances to other transmitters to limit cognitive outages occurring due to mutual interference. If a cognitive transmitter detects that another user is occupying the spectrum within a certain region around it (contention region), it'll refrain from transmitting. Otherwise, it may transmit depending on other factors such as receiver availability, cut-off thresholds, etc. Such methods are similar to CSMA/CA employed in IEEE 802.11 [13]. The transmitting cognitive nodes follow a Matern-hardcore point process which may be analyzed based on the techniques adopted in [13], [46], [47]. However, the discussion of such schemes is out of the scope of the paper.

III. Interference Analysis

This section derives the MGF and mean of I under several transmission schemes for cognitive nodes, where I is the aggregate interference (5).

The MGF of the aggregate interference is defined as $M_I(s) = E[e^{-sI}]$ [18], [19]. Let $M_{I_i}(s)$ define the MGF of I_i. Because of the independence, the MGF given N transmitters can be written as $M_{I/N}(s) = (M_{I_i}(s))^N$. Averaging with respect to the Poisson model (1) yields [19], [25]

$$M_I(s) = e^{\lambda_t A_t \left(M_{I_i}(s)-1\right)}. \tag{7}$$

Our objective now is to find $M_{I_i}(s)$ under the following schemes.

A. Nearest association

Four nearest association based transmit power control schemes are developed next.

1) Scheme 1 (Nearest association and path loss inversion): The transmitter connects to the nearest receiver ($\phi_{r,1\backslash i}$), and transmits at a power level sufficient to ensure a constant received power when averaged over small scale fading. This scheme is used extensively in the CDMA uplink to compensate the near-far problem [8], where all transmitters adjust their power such that the received power at the base station from each of them is the same.

Suppose P_s is the average received power[1] ensured, and r_c is the distance to the nearest receiver from $\phi_{t,i}$. Let $|g_i|^2$ be the channel gain from $\phi_{t,i}$ to its associated receiver. We need $P_s = E_{|g_i|^2}[P_i|g_i|^2 r_c^{-\alpha}]$. Therefore, the transmit power level of $\phi_{t,i}$, $P_i = P_s r_c^{\alpha}$. Substituting P_i in (4), it is possible to write $M_{I_i}(s)$ as [25]

$$\begin{aligned} M_{I_i}(s) &= E_{|h_i|^2, r_i, r_c}[e^{-sI_i}] \\ &= E_{r_c}[E_{r_i}[E_{|h_i|^2}[e^{-sP_s r_c^{\alpha} r_i^{-\alpha}|h_i|^2}]]], \end{aligned} \tag{8}$$

due to the independence of $|h_i|^2$, r_c, and r_i.

[1] The average received power will be the receiver sensitivity plus an appropriate fade margin.

To evaluate (8), we use a series summation based approach utilizing the fact that $(1+x)^{-1} = \sum_{k=0}^{\infty}(-x)^k$ when $|x| < 1$. $M_{I_i}(s)$ can thus be written as

$$M_{I_i}(s) = \int_0^{\infty} \int_{R_g}^{R_e} \sum_{t=0}^{\infty} (-sP_s r_c^{\alpha} r_i^{-\alpha})^t f_{r_i}(r_i) f_{r_c}(r_c) dr_i dr_c. \tag{9}$$

Averaging (9) with respect to r_i and r_c gives us

$$\begin{aligned} M_{I_i}(s) = &\frac{2\pi}{A_t} \sum_{t=0}^{\infty} (\pi\lambda_r)^{-\frac{\alpha t}{2}} (-sP_s)^t \\ &\times \left(\frac{R_e^{2-\alpha t} - R_g^{2-\alpha t}}{2-\alpha t} \right) \Gamma(\frac{\alpha t}{2}+1), \alpha > 2. \end{aligned} \tag{10}$$

The infinite sum in (10) converges as a rule of thumb when $sP_s < 0.1$. This condition is satisfied for practical system parameters as will be seen in Section V. Moreover, the series summation based approach renders the moments readily.

From $M_{I_i}(s)$, we can find the moments of the aggregate interference readily. For example, the mean aggregate interference $E[I] = \lambda_t A_t E[I_i]$, where $E[I_i] = -\frac{d}{ds} M_{I_i}(s)|_{s=0}$. Therefore, $E[I]$ is found to be

$$E[I] = 2\pi\lambda_t P_s (\pi\lambda_r)^{-\frac{\alpha}{2}} \left(\frac{R_e^{2-\alpha} - R_g^{2-\alpha}}{2-\alpha} \right) \Gamma(\frac{\alpha}{2}+1), \alpha \neq 2. \tag{11}$$

When $\alpha \to 2$, $E[I]$ can be obtained after applying the L'Hospital's rule to (11) as

$$E[I]|_{\alpha \to 2} = \frac{4\pi\lambda_t P_s}{\pi\lambda_r} (\log R_e - \log R_g). \tag{12}$$

2) Scheme 2 (Nearest association and path loss inversion with a cut-off power level): In Scheme 1, the cognitive transmit power can go arbitrarily high. When that happens, the resulting interference is unconstrained. This situation can be avoided by enforcing a cut-off power level [13]. Thus, Scheme 2 enforces an added constraint of a cut-off power level P_c, and if a cognitive node needs more power than P_c, it will abort transmission.

Now, the interference from the $\phi_{t,i}$ (4) becomes $I_i = Q_i P_i |h_i|^2 r_i^{-\alpha}$, where $Q_i = \text{Bernoulli}(q_i)$ with $q_i = \Pr[P_i < P_c] = \Pr[P_s r_c^{\alpha} < P_c] = 1 - e^{-\pi\lambda_r \left(\frac{P_c}{P_s}\right)^{\frac{2}{\alpha}}}$. We can now write

$$\begin{aligned} M_{I_i}(s) = 1 - q_i + &\frac{2\pi^2\lambda_r}{A_t} \int_0^{\left(\frac{P_c}{P_s}\right)^{\frac{1}{\alpha}}} r_c e^{-\pi\lambda_r r_c^2} \\ &\times \left((\mathcal{V}(R_g) - 1) R_g^2 - (\mathcal{V}(R_e) - 1) R_e^2 \right) dr_c, \end{aligned} \tag{13}$$

with $\mathcal{V}(x) = {}_2F_1\left(1, \frac{2}{\alpha}; 1+\frac{2}{\alpha}, -\frac{x^{\alpha}}{sP_s r_c^{\alpha}}\right)$. As performed in Scheme 1, we can use a series expansion, and average $M_{I_i}(s)$

to get a closed-form solution. It thus becomes

$$M_{I_i}(s) = 1 - q_i + q_i \sum_{t=0}^{\infty} (-sP_s)^t \left(\frac{2\pi}{A_t} \int_{R_g}^{R_e} r_i^{1-\alpha t} dr_i \right) \times \left(\frac{2\pi\lambda_r}{q_i} \int_0^{\left(\frac{P_c}{P_s}\right)^{\frac{1}{\alpha}}} r_c^{1+\alpha t} e^{-\pi\lambda_r r_c^2} dr_c \right)$$
$$= e^{-\pi\lambda_r \left(\frac{P_c}{P_s}\right)^{\frac{2}{\alpha}}} + \frac{2\pi}{A_t} \sum_{t=0}^{\infty} \left(-\frac{sP_s}{\pi^{\frac{\alpha}{2}} \lambda_r^{\frac{\alpha}{2}}} \right)^t \times \left(\frac{R_e^{2-\alpha t} - R_g^{2-\alpha t}}{2-\alpha t} \right) \left(\Gamma\left(\frac{\alpha t}{2}+1\right) - \Gamma\left(\frac{\alpha t}{2}+1, \pi\lambda_r \left(\frac{P_c}{P_s}\right)^{\frac{2}{\alpha}}\right) \right), \alpha > 2. \quad (14)$$

Similar to Scheme 1, we can obtain $E[I]$ as

$$E[I] = 2\pi\lambda_t P_s (\pi\lambda_r)^{-\frac{\alpha}{2}} \left(\frac{R_e^{2-\alpha} - R_g^{2-\alpha}}{2-\alpha} \right) \left(\Gamma\left(\frac{\alpha}{2}+1\right) - \Gamma\left(\frac{\alpha}{2}+1, \pi\lambda_r \left(\frac{P_c}{P_s}\right)^{\frac{2}{\alpha}}\right) \right), \alpha \neq 2. \quad (15)$$

3) Scheme 3 (Nearest-M association and path loss inversion with a cut-off power level): Schemes 1 and 2 assume the nearest receiver is always available for reception, which however may not be ready at a given time. Scheme 3 allows a transmitter to scan up to the M-th nearest receiver ($\phi_{r,M\backslash i}$) whenever necessary [14]. To analyze this scheme, we denote the probability that a receiver is available with β_r, and this probability is constant for all receivers. Moreover, the availabilities of receivers are mutually independent events.

In this scheme, each transmitter node attempts to connect to the nearest receiver. However, if this fails, a connection is attempted with the next nearest and so on till M nearest receivers are scanned, or the transmission attempt is aborted. If a successful association is made, a constant averaged received power of P_s to that receiver must be guaranteed. However, if this guarantee makes the transmit power exceed P_c, the transmission does not take place. Moreover, if the required transmit power exceeds the cut-off level for the $\phi_{r,k\backslash i}$ ($k < M$), no further association attempts are made with the rest of the receivers. This is because $P_s r_{c,k}^{\alpha} > P_c$ implies that $P_s r_{c,k+1}^{\alpha} > P_c$, where $r_{c,k}$ denotes the distance from $\phi_{t,i}$ to $\phi_{r,k\backslash i}$.

The interference from $\phi_{t,i}$ (4) is expressed as $I_i = W_i P_i |h_i|^2 r_i^{-\alpha}$. W_i is a Bernoulli random variable similar to Q_i of Scheme 2 with a success probability (probability of transmission) of w_i. This probability depends on the availability of a receiver β_r, the number of nearest receivers a transmitter is allowed an association attempt M, and the cut-off power level P_c. Thus, the success probability w_i can be written as [48]

$$w_i = \beta_r \sum_{k=1}^{M} (1-\beta_r)^{k-1} p_k, \quad (16)$$

where p_k is the probability that the transmit power of a transmitter associated with $\phi_{r,k\backslash i}$ is below the cut-off level P_c. This probability is thus written as $p_k = \Pr[P_s r_{c,k}^{\alpha} < P_c]$. Using the distribution of $r_{c,k}$ (3), p_k is found to be [48]

$$p_k = 1 - \frac{\Gamma\left(k, \pi\lambda_r \left(\frac{P_c}{P_s}\right)^{\frac{2}{\alpha}}\right)}{(k-1)!}. \quad (17)$$

Now, the simplified MGF of the interference from $\phi_{t,i}$ ($M_{I_i}(s)$) can be obtained in a similar way to Scheme 2 using the series summation based approach as

$$M_{I_i}(s) = 1 - \beta_r \sum_{k=1}^{M} (1-\beta_r)^{k-1} \left(1 - \frac{\Gamma\left(k, \pi\lambda_r \left(\frac{P_c}{P_s}\right)^{\frac{2}{\alpha}}\right)}{(k-1)!} \right) + \frac{2\pi}{A_t} \sum_{t=0}^{\infty} \left(-\frac{sP_s}{\pi^{\frac{\alpha}{2}} \lambda_r^{\frac{\alpha}{2}}}\right)^t \left(\frac{R_e^{2-\alpha t} - R_g^{2-\alpha t}}{2-\alpha t} \right) \times \sum_{k=1}^{M} \frac{\beta_r (1-\beta_r)^{k-1}}{(k-1)!} \left(\Gamma\left(\frac{\alpha t}{2}+k\right) - \Gamma\left(\frac{\alpha t}{2}+k, \pi\lambda_r \left(\frac{P_c}{P_s}\right)^{\frac{2}{\alpha}}\right) \right), \alpha > 2. \quad (18)$$

$E[I]$ can be obtained as

$$E[I] = 2\pi\lambda_t P_s (\pi\lambda_r)^{-\frac{\alpha}{2}} \left(\frac{R_e^{2-\alpha} - R_g^{2-\alpha}}{2-\alpha} \right) \times \sum_{k=1}^{M} \frac{\beta_r (1-\beta_r)^{k-1}}{(k-1)!} \left(\Gamma\left(\frac{\alpha}{2}+k\right) - \Gamma\left(\frac{\alpha}{2}+k, \pi\lambda_r \left(\frac{P_c}{P_s}\right)^{\frac{2}{\alpha}}\right) \right), \alpha \neq 2. \quad (19)$$

4) Scheme 4 (Nearest association and path loss inversion with a location dependent cut-off power level): In schemes 2 and 3, the cut-off transmit power P_c is a constant. We will now consider the case where P_c depends on r_i and α, and has the form $P_c = P_I r_i^{\alpha}$ for $\phi_{t,i}$, where P_I is a constant threshold value. The distance to the primary receiver (r_i) can be obtained through periodic acknowledgement signals from it [6].

The probability of $P_i < P_c$ (q_i) would thus be $1 - e^{-\pi\lambda_r r_i^2 \left(\frac{P_I}{P_s}\right)^{\frac{2}{\alpha}}}$. By employing a similar method to the derivation of $M_{I_i}(s)$ in Scheme 2, we can write $M_{I_i}(s)$ for Scheme 3 as

$$M_{I_i}(s) = E_{r_i} \left[e^{-\pi\lambda_r r_i^2 \left(\frac{P_I}{P_s}\right)^{\frac{2}{\alpha}}} + \sum_{t=0}^{\infty} \left(-\frac{sP_s}{\pi^{\frac{\alpha}{2}} \lambda_r^{\frac{\alpha}{2}}} \right)^t r_i^{-\alpha t} \times \left(\Gamma\left(\frac{\alpha t}{2}+1\right) - \Gamma\left(\frac{\alpha t}{2}+1, \pi\lambda_r r_i^2 \left(\frac{P_I}{P_s}\right)^{\frac{2}{\alpha}}\right) \right) \right]. \quad (20)$$

After performing the expectation, $M_{I_i}(s)$ can be expressed as

$$M_{I_i}(s) = \frac{2\pi}{A_t}\Bigg(\frac{e^{-\pi\lambda_r\left(\frac{P_I}{P_s}\right)^{\frac{2}{\alpha}}R_g^2} - e^{-\pi\lambda_r\left(\frac{P_I}{P_s}\right)^{\frac{2}{\alpha}}R_e^2}}{2\pi\lambda_r\left(\frac{P_I}{P_s}\right)^{\frac{2}{\alpha}}} + \sum_{t=0}^{\infty}\left(-\frac{sP_s}{\pi^{\frac{\alpha}{2}}\lambda_r^{\frac{\alpha}{2}}}\right)^t\Bigg(\left(\frac{R_e^{2-\alpha t}-R_g^{2-\alpha t}}{2-\alpha t}\right)\Gamma\left(\frac{\alpha t}{2}+1\right) - \left(\mathcal{W}(R_e,t)\mathcal{W}(R_g,t)\right)\Bigg)\Bigg), \alpha > 2, \quad (21)$$

where $\mathcal{W}(x,t)$ is given by

$$\mathcal{W}(x,t) = \frac{e^{-\pi\lambda_r x^2\left(\frac{P_I}{P_s}\right)^{\frac{2}{\alpha}}}}{\alpha t - 2}\left((\pi\lambda_r)^{\frac{\alpha t}{2}-1}\left(\frac{P_I}{P_s}\right)^{t-\frac{2}{\alpha}} \times\left(\pi\lambda_r x^2\left(\frac{P_I}{P_s}\right)^{\frac{2}{\alpha}}+1\right) - x^{2-\alpha t}e^{\pi\lambda_r x^2\left(\frac{P_I}{P_s}\right)^{\frac{2}{\alpha}}} \times\Gamma\left(\frac{\alpha t}{2}+1, \pi\lambda_r x^2\left(\frac{P_I}{P_s}\right)^{\frac{2}{\alpha}}\right)\right). \quad (22)$$

The mean of the aggregate interference is found in a similar manner to the above schemes as

$$E[I] = \frac{2\pi\lambda_t P_s}{\pi^{\frac{\alpha}{2}}\lambda_r^{\frac{\alpha}{2}}}\left(\left(\frac{R_e^{2-\alpha}-R_g^{2-\alpha}}{2-\alpha}\right)\Gamma\left(\frac{\alpha}{2}+1\right) - \left(\mathcal{W}(R_e,1)-\mathcal{W}(R_g,1)\right)\right), \alpha \neq 2. \quad (23)$$

Moreover, the average probability of a cognitive transmitter node being allowed to transmit $q_i = 1 - \frac{2\pi}{A_t}\left(\frac{e^{-\pi\lambda_r\left(\frac{P_I}{P_s}\right)^{\frac{2}{\alpha}}R_g^2} - e^{-\pi\lambda_r\left(\frac{P_I}{P_s}\right)^{\frac{2}{\alpha}}R_e^2}}{2\pi\lambda_r\left(\frac{P_I}{P_s}\right)^{\frac{2}{\alpha}}}\right)$.

B. Best-received-power association

This subsection develops and analyzes transmission schemes based on highest received power association.

1) Scheme 5 (Best received power association and channel inversion with a cut-off power level): In this scheme, a transmitter first selects the receiver $\phi_{r,p\setminus i}$ with the highest instantaneous received power, and inverts the channel gain. However, this process needs the CSI and the link distance, which the transmitter utilizes to ensure an average received power of P_s at the selected receiver. However, if the required transmit power exceeds the cut-off P_c, the transmission attempt would be aborted. The major advantage of this scheme over Scheme 2 employing nearest association and path loss inversion is that it guarantees the lowest required transmit power for any given P_s.

However, the analysis is complicated because of the need for the probability distribution of the distance to the receiver having the highest instantaneous received power. The detailed analysis is provided in Appendix I and II. The MGF $M_{I_i}(s)$ is obtained as

$$M_{I_i}(s) = e^{-\pi\lambda_r\Gamma(\frac{2}{\alpha}+1)\left(\frac{P_c}{P_s}\right)^{\frac{2}{\alpha}}} + \frac{2\pi}{A_t}\sum_{t=0}^{\infty}\left(\frac{-sP_s}{(\pi\lambda_r\Gamma(\frac{2}{\alpha}+1))^{\frac{\alpha}{2}}}\right)^t \times\left(\frac{R_e^{2-\alpha t}-R_g^{2-\alpha t}}{2-\alpha t}\right)\left(\Gamma\left(\frac{\alpha t}{2}+1\right) - \Gamma\left(\frac{\alpha t}{2}+1, \pi\lambda_r\Gamma(\frac{2}{\alpha}+1)\left(\frac{P_c}{P_s}\right)^{\frac{2}{\alpha}}\right)\right), \alpha > 2. \quad (24)$$

The average aggregate interference $E[I]$ is derived as

$$E[I] = 2\pi\lambda_t P_s\left(\pi\lambda_r\Gamma(\frac{2}{\alpha}+1)\right)^{-\frac{\alpha}{2}}\left(\frac{R_e^{2-\alpha}-R_g^{2-\alpha}}{2-\alpha}\right) \times\left(\Gamma\left(\frac{\alpha}{2}+1\right) - \Gamma\left(\frac{\alpha}{2}+1, \pi\lambda_r\Gamma(\frac{2}{\alpha}+1)\left(\frac{P_c}{P_s}\right)^{\frac{2}{\alpha}}\right)\right), \alpha \neq 2. \quad (25)$$

It should be noted that this scheme can be generalized where each receiver has a probability of not being available (β_r), and a transmitter attempts to connect to the M receivers providing the best received power. This generalization could be done similar to Scheme 3.

2) Scheme 6 (Best received power association and constant transmit power with self deactivation based on estimated cognitive receiver received power): This scheme selects $\phi_{r,p\setminus i}$ to associate, but avoids transmitter side power control. Instead, a constant power level of $P_T(\leq P_c)$ is utilized provided the received power of a cognitive receiver does not to fall below the required threshold of P_s. Otherwise, transmission is aborted.

The interference from $\phi_{t,i}$ (4) can be written as $I_i = V_i P_T|h_i|^2 r_i^{-\alpha}$, where $V_i = \text{Bernoulli}(v_i)$ with $v_i = \Pr[P_{rec} > P_s]$. P_{rec} is the received power at the receiver having the best instantaneous received power. In order to find v_i, we will employ the result (35) in Scheme 4 obtained using PPP mapping. As such, P_{rec} is written as $P_{rec} = P_T r_p^{-1}$. Then,

$$v_i = \Pr[P_T r_p^{-1} > P_s] = 1 - e^{-\pi\lambda_r\Gamma(\frac{2}{\alpha}+1)\left(\frac{P_T}{P_s}\right)^{\frac{2}{\alpha}}}.$$

The interference from a single transmitter $M_{I_i}(s)$ can be written as

$$M_{I_i}(s) = 1 - v_i + \frac{v_i\pi}{A_t}\left((\mathcal{Y}(R_g)-1)R_g^2 - (\mathcal{Y}(R_e)-1)R_e^2\right), \quad (26)$$

where $\mathcal{Y}(x) = {}_2F_1\left(1, \frac{2}{\alpha}; 1+\frac{2}{\alpha}, -\frac{x^\alpha}{sP_T}\right)$. An expression for $M_{I_i}(s)$ can also be derived from the series summation based approach as

$$M_{I_i}(s) = e^{-\pi\lambda_r\Gamma(\frac{2}{\alpha}+1)\left(\frac{P_T}{P_s}\right)^{\frac{2}{\alpha}}} + \left(1 - e^{-\pi\lambda_r\Gamma(\frac{2}{\alpha}+1)\left(\frac{P_T}{P_s}\right)^{\frac{2}{\alpha}}}\right) \times\sum_{t=0}^{\infty}(-sP_T)^t\frac{2\pi}{A_t}\left(\frac{R_e^{2-\alpha t}-R_g^{2-\alpha t}}{2-\alpha t}\right), \alpha > 2. \quad (27)$$

The average aggregate interference thus becomes

$$E[I] = 2\pi\lambda_t P_T \left(1 - e^{-\pi\lambda_r\Gamma(\frac{2}{\alpha}+1)\left(\frac{P_T}{P_s}\right)^{\frac{2}{\alpha}}}\right) \times \left(\frac{R_e^{2-\alpha} - R_g^{2-\alpha}}{2-\alpha}\right), \alpha \neq 2. \quad (28)$$

Similar to Scheme 3, a generalization is also possible for this scheme.

C. Transmission restrictions based on node locations

We now develop a scheme based on restricting transmissions of a secondary transmitter node based on other secondary node locations, where the scheme considers the distance to receivers. However, many other variants can be introduced by combining the schemes mentioned before.

1) Scheme 7 (Nearest-M association and path loss inversion with a maximum association radius): An area of radius d_{CRR} around each cognitive transmitter is considered as the association region. The association region radius would be initially set as a system parameter taking into account the interference constraints of the primary receiver. Moreover, there would be no cut-off power level (P_c).

A secondary transmitter checks the presence of any receivers within the association region, and may transmit if there are one or more receivers. If there are, it would select the nearest receiver. If that receiver is available (with a probability of β_r), transmission is made. The transmit power is adjusted to ensure a constant average received power (P_s). However, this receiver may not be available (with a probability of $1-\beta_r$). Then, the cognitive transmitter checks whether there are more receivers within the association region. If so, the second nearest one is selected, and an association is made if that receiver is available. This process continues for T times where $T = \min(M, \text{number of receivers})$.

Let the interference from $\phi_{t,i}$ be $I_i = S_i P_i |h_i|^2 r_i^{-\alpha}$, where $S_i = \text{Bernoulli}(s_i)$ with

$$s_i = \beta_r \sum_{k=1}^{M} (1-\beta_r)^{k-1} (1 - \rho_{k-1} - \rho_{k-2} \dots \rho_0).$$

The parameter ρ_{k-1} denotes the probability that there are exactly $k-1$ nodes within the association region given by $\rho_{k-1} = \frac{(\lambda_r \pi d_{CRR}^2)^{k-1}}{(k-1)!} e^{-\lambda_r \pi d_{CRR}^2}, \quad k = 1, 2, \dots M$. Using this, s_i can be simplified as

$$s_i = \beta_r \sum_{k=1}^{M} (1-\beta_r)^{k-1} \left(1 - \frac{\Gamma\left(k, \pi\lambda_r d_{CRR}^2\right)}{(k-1)!}\right).$$

We see that the expression for s_i is analogous to the expression for w_i obtained in Scheme 3, with d_{CRR} replacing $\left(\frac{P_c}{P_s}\right)^{\frac{1}{\alpha}}$. This observation is logically consistent because an association region would bar transmissions to receivers farther than a certain distance. This is effectively enforcing a cut-off power level in a different way. Equations for $M_{I_i}(s)$ and $E[I]$ would thus be similar to Scheme 3, with d_{CRR} instead $\left(\frac{P_c}{P_s}\right)^{\frac{1}{\alpha}}$.

Remark 1: This scheme is analogous to Scheme 2 (Nearest association and path loss inversion with a cut-off power level).

D. Iterative schemes

Iterative schemes utilize system feedback to reduce the primary outage and the probability of cognitive transmitter cut-off. Furthermore, when the primary outage is significantly low, there is room for either more cognitive transmitters or for the existing cognitive transmitters to be allowed to transmit at a higher power. Iterative power control schemes are suitable in this context. Considering per-user power control schemes, the best system parameter to change according to primary system requirements is the cut-off power level P_c. The value for P_c may be calculated and disseminated by a central controller for the cognitive system, or generated by each cognitive transmitter individually.

As the cognitive users are scavenging spectrum from the primary system, the primary system's performance becomes the first priority. Therefore, only while the target for the primary receiver's performance is met, can the cognitive network's performance be increased. With this principle, the proposed iterative scheme is explained in the next paragraph.

We must ensure that the PR outage is less than a predetermined level $P_{OUT,max}$. However, while this requirement is fulfilled, the cognitive transmitter availability can be increased by increasing the cut-off power level P_c in small steps. This process happens iteratively till P_c is increased by the maximum amount while still keeping the PR outage below the threshold. Conversely, when the PR outage is above $P_{OUT,max}$, P_c is reduced iteratively. The initial value for P_c can be any reasonable value. Once the final P_c has been decided through the iterations, the cognitive transmitters can employ a power control scheme mentioned in the previous sections. Moreover, even after a suitable value for P_c is established, the iteration process should be repeated every T seconds as channel conditions may have changed.

IV. Primary Receiver Outage Analysis

We will derive the CDF of the signal to interference and noise ratio (SINR) of the PR in this section. A simple variable substitution of the CDF gives the outage probability.

The primary transmitter is located at a distance R from the primary receiver (Fig. 1), and has a power level of P_p. The primary signals are also assumed to undergo Rayleigh fading and path-loss. Therefore, the received power (P_R) at the primary receiver can be written as [19], [25]

$$P_R = P_p R^{-\alpha} |h|^2, \quad (29)$$

where $|h|^2$ is the channel power gain. For a Rayleigh fading environment, $|h|^2$ is exponentially distributed. Let σ_n^2 denote the noise variance. The, SINR γ can be written as $\gamma = \frac{P_p R^{-\alpha}|h|^2}{I+\sigma_n^2}$. It is possible to obtain the CDF of the SINR as [18]

$$F_\gamma(x) = 1 - e^{\left(-\frac{x\sigma_n^2}{P_p R^{-\alpha}}\right)} M_I\left(\frac{x}{P_p R^{-\alpha}}\right). \quad (30)$$

Substituting the required threshold SINR (γ_{th}) for x yields the outage.

A. Primary transmitters form a PPP

The outage (30) was derived for a single primary transmitter at a fixed distance from the PR. However, in practice, there will be multiple primary transmitters which can be modeled as a PPP. We then extend the outage result (30) to this scenario. In this case, all transmitters other than the one associated with the receiver will cause interference.

When the primary transmitters form a PPP in $\mathbb{R}^2$, we assume that the PR is associated to the nearest primary transmitter. The transmitter will be employing a power control scheme to ensure a constant average received power at the PR ($P_{c,PR}$). Therefore, the received power at the PR (P_R) becomes $P_R = P_{c,PR}|h|^2$. The SINR is written as $\gamma = \frac{P_{c,PR}|h|^2}{I+I_p+\sigma_n^2}$, where I_p is the aggregate interference from other primary transmitters. The CDF of the SINR is obtained as [18]

$$F_\gamma(x) = 1 - e^{\left(-\frac{x\sigma_n^2}{P_{c,PR}}\right)} M_I\left(\frac{x}{P_{c,PR}}\right) M_{I_p}\left(\frac{x}{P_{c,PR}}\right). \quad (31)$$

Let the field of interfering primary transmitters (apart from the associated transmitter) be ψ_p. Although each receiver is connected to the closest transmitter, in the perspective of the transmitter, the receiver may not be the one closest to it. Contrary to a cognitive network, the receivers would be the entities initiating a request in the primary network (note that the primary network would be fundamentally different from the cognitive network). Moreover, as the downlink is considered, the transmitter may be connected to multiple receivers employing different multiplexing schemes. Therefore, the best option is to assume a fixed power level which will be the maximum transmit power giving a worst case scenario. Let this power level be $P_{p,PT}$, the distance to the closest primary transmitter $r_{c,p}$, the distance from the PR to the j-th primary transmitter be R_j, and the density of the primary transmitters be λ_p. Then, $I_p = \sum_{j\in\psi_p} P_{p,PT}|h_j|^2 R_j^{-\alpha}$ [18].

Using the Campbell's theorem [36], $M_{I_p}(s)$ is written as [18]

$$\begin{aligned} M_{I_p}(s) &= e^{\left(\int_{r_{c,p}}^{\infty} E\left[e^{-sP_{p,PT}|h_j|^2 R_j^{-\alpha}} - 1\right] 2\pi\lambda_p R_j dR_j\right)} \\ &= e^{E_{r_{c,p}}\left[\frac{2\pi\lambda_p s P_{p,PT} r_{c,p}^{2-\alpha} {}_2F_1\left(1,1-\frac{2}{\alpha};2-\frac{2}{\alpha},-\frac{sP_{p,PT}}{r_{c,p}^{\alpha}}\right)}{2-\alpha}\right]} \\ &\qquad\qquad , \alpha \neq 2, \end{aligned} \quad (32)$$

where the result holds for $\alpha > 2$. The distribution of $r_{c,p}$ follows equation (3) with λ_p instead of λ_r, and the expectation can be computed numerically.

V. Numerical Results

This section shows the outage probability, mean aggregate interference, and the cognitive cut-off probability. We will use the parameters $R_g = 20$, $R_e = 100$, $R = 30$, and $\gamma_{th} = 1$. To highlight the effects of interference, the additive noise variance σ_n^2 is set to 0. Moreover, for comparison purposes, we will use the value for P_c for the transmit power of Scheme 6 (P_T).

A. Nearest association and highest-received-power association: Impact of primary transmit power

We will first investigate the impact of the primary transmit power P_p on the primary outage for the different power control and receiver association schemes.

Fig. 2 plots the PR outage as a function of primary transmit power level P_p for Scheme 4. The theoretical results match perfectly with the simulation. The outage reduces with respect to P_p as expected. We see that the primary outage depends inversely with P_I. However, with regards to α, the performance diminishes with its increase. Although we would expect that a higher α would attenuate the interfering cognitive signals, it also means that the received primary power level is also low. Moreover, when α is high, the transmit power of a cognitive transmitter would also increase to ensure a constant average cognitive receiver received power (P_s).

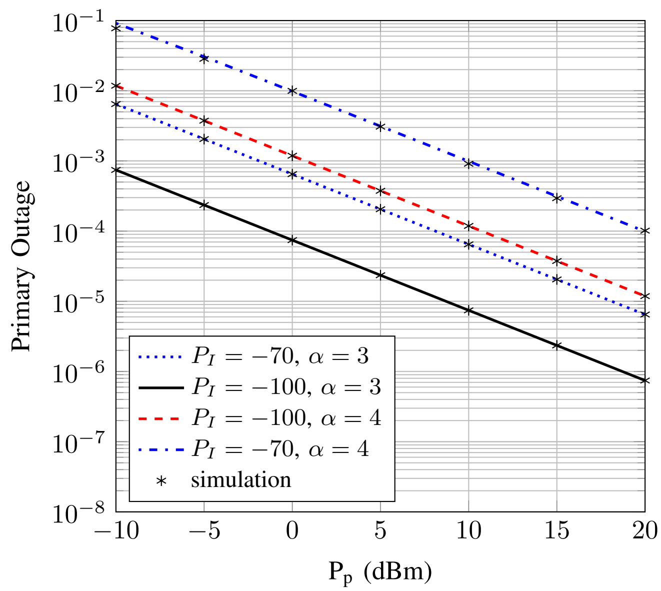

Fig. 2: Scheme 4: The PR outage probability vs the primary power level P_p for different values of P_I (dBm), and α. $\lambda_t = 5\times10^{-3}$, $P_s = -80$ dBm, and $\lambda_r = 2.5\times10^{-3}$.

The PR outage vs the primary transmit power level P_p for Schemes 1, 2, 5, and 6 are plotted in Fig. 3. We observe that Scheme 1 results in the worst outage under the given system parameters. Scheme 6 only provides a marginally better performance. Both Schemes 2 and 5 ensure a significantly lower PR outage. Although the plots for Schemes 2 and 5 overlap, the PR outage for Scheme 5 is slightly lower. This is because although the individual cognitive transmit powers for Scheme 5 may be higher than those of Scheme 2, cognitive transmitters of Scheme 5 are more likely to be cut-off from transmission (due to the cut-off power level P_c).

B. Nearest association and highest-received-power association: Impact of cognitive system thresholds

We will now investigate the effect of the cut-off power threshold P_c and the average received power level of a cognitive receiver (P_s) on the primary outage, mean I on the primary receiver, and the cognitive cut-off probability.

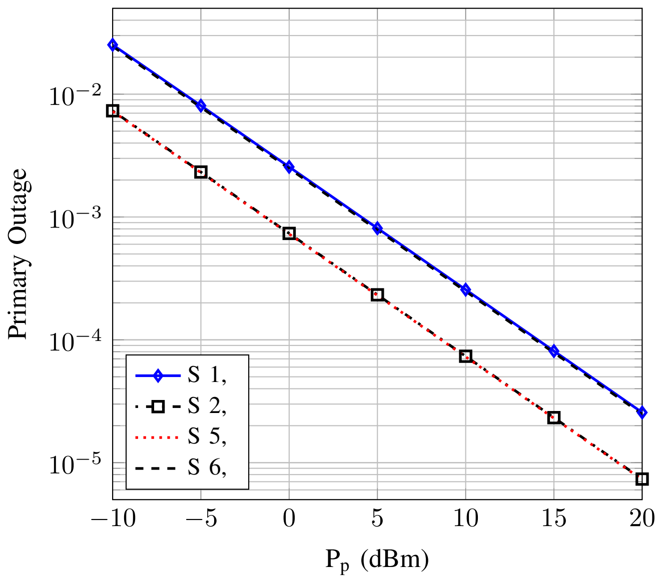

Fig. 3: Schemes 1, 2, 5, and 6: The outage probability vs the primary power level P_p. $\lambda_t = 5 \times 10^{-3}$, $\lambda_r = 1 \times 10^{-3}$, $P_c = -40$ dBm, $P_s = -80$ dBm, and $\alpha = 3$.

The primary outage probability under Scheme 2 is plotted over the cognitive transmitter cut-off power threshold P_c in Fig. 4. Naturally, we would expect the outage to increase as P_c increases. However, the outage increases initially, and then flattens out. This is because at higher cut-off levels, almost all the cognitive transmit powers would fall below the threshold. Moreover, the rate of outage increase before flattening out depends on the cognitive receiver density λ_r. The cognitive transmitter density λ_t only introduces a shift to the curves, and does not affect the shape.

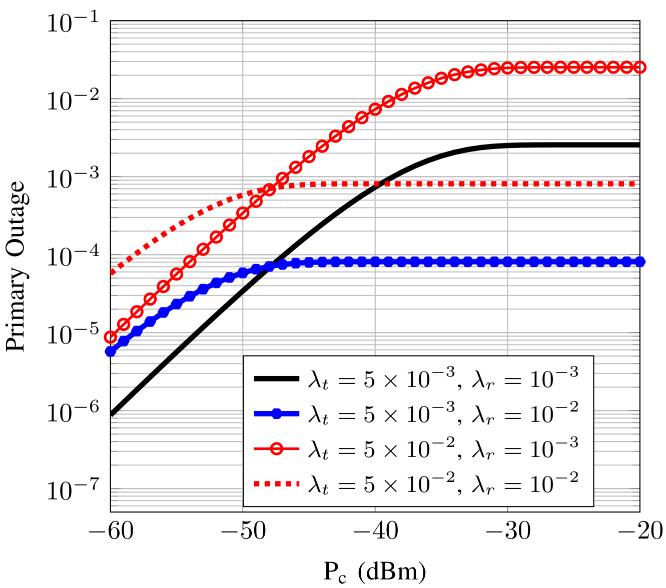

Fig. 4: Scheme 2: The PR outage probability vs the cut-off threshold P_c for different values of λ_t, and λ_r. $\alpha = 3$, $P_p = 0$ dBm, and $P_s = -80$ dBm.

Fig. 5 plots the mean aggregate interference power of the schemes with respect to the average received power level of a cognitive receiver (P_s). Scheme 1 shows a constant increase of the interference power with respect to P_s, and thus provides the highest interference at high P_s. Scheme 6 has the highest mean aggregate interference at low P_s. The level keeps constant initially as P_s rises, but starts to drop after a certain point due to cognitive transmitters getting cut-off from transmission. For Schemes 2, 4, and 5, there exists a maxima when the mean interference is at its highest. For these schemes, when the average received cognitive receiver power is low, the transmit powers of the cognitive transmitters are low, and thus results in a low interference. When P_s increases, the cognitive transmit powers would increase, and in turn the interference would increase. However, as P_s increases even further, the number of cognitive transmitters getting cut-off due to having a transmit power greater than the cut-off level P_c would increase. Therefore, this reduction in transmitting cognitive nodes leads to a lower aggregate interference, and thus the maxima occurs. The value of P_s when the maxima occurs is dependent on several factors, and can be obtained through differentiation by using the derived equations for $E[I]$. Moreover, as P_s increases, Scheme 4 can generate a slightly higher mean aggregate interference to the PR compared to Schemes 2 and 5, whereas the opposite is true for lower P_s. Again, the curves for Schemes 2 and 5 are almost the same. However, Scheme 2 has a slightly higher aggregate interference at higher P_s.

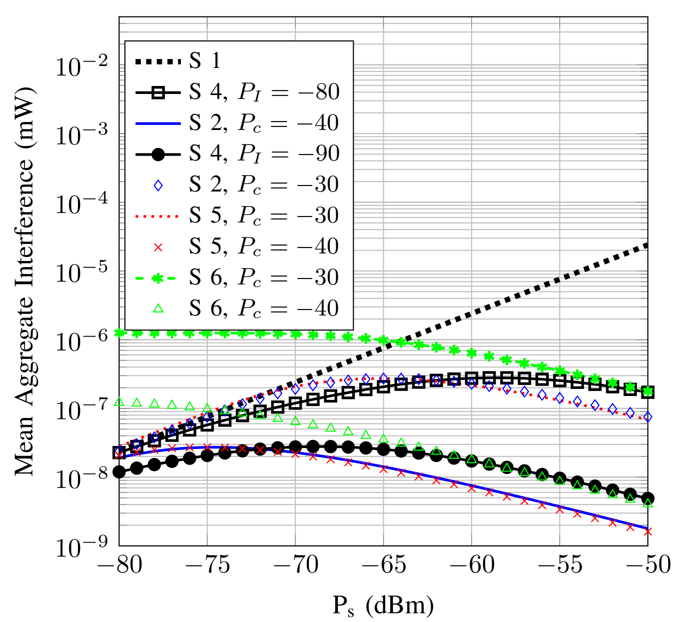

Fig. 5: Schemes 1, 2, 4, 5, and 6: The mean aggregate interference vs the average received cognitive power P_s under different P_c (dBm) and P_I (dBm). $\alpha = 3$, $\lambda_t = 5 \times 10^{-3}$, and $\lambda_r = 2.5 \times 10^{-3}$.

It is important to gain an understanding on the impact of different power control schemes on the cognitive system. Fig. 6 plots the probability that a cognitive transmitter is cut-off from transmission with respect to the average received cognitive receiver power P_s, for Schemes 2 and 5. For Scheme 1, this probability is 0, and for Scheme 6, this probability is same as Scheme 5 (we are using the value for P_c in P_T).

For a high cognitive receiver density λ_r, the curves show a sharp drop-off under higher P_c when P_s is low. The cut-off probability for Scheme 2 is always lower than Scheme 5. In Fig. 5 and 3, it was observed that the mean interference and the primary outage were slightly lower for Scheme 5. Thus, a trade-off exists in the primary and cognitive performance. The curves for Scheme 4 would behave in a similar manner for appropriate values for P_I instead of P_c. To conclude, a high cognitive receiver density, a low average received cognitive receiver power P_s, and a higher value for the threshold P_c reduce the probability that a cognitive transmitter is cut-off from transmitting.

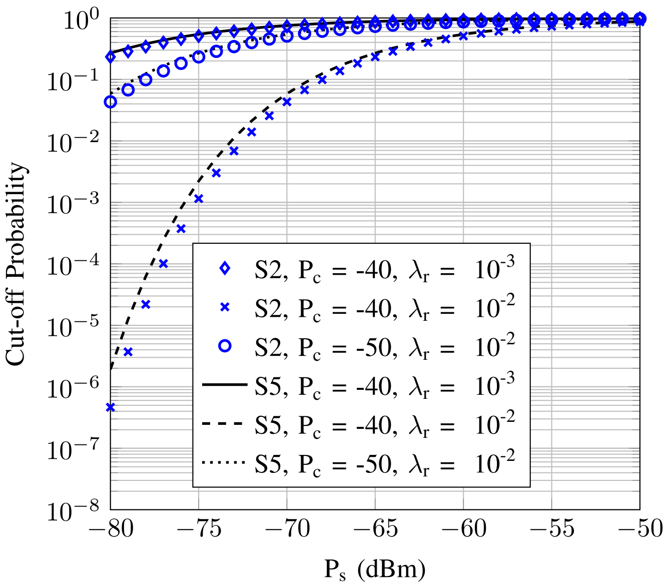

Fig. 6: Schemes 2 and 5: The average probability of a cognitive transmitter being cut-off from transmission vs P_s for different λ_r and P_c (dBm). $\alpha = 3$.

C. Nearest-M association

We will now investigate the performance of Scheme 3, where the transmitter can attempt to connect with the M nearest receivers. Fig. 7 plots the primary receiver outage vs the availability of a cognitive receiver (β_r). The base curve has parameters of $M = 10$, $\lambda_r = 1 \times 10^{-3}$, and $P_s = 1 \times 10^{-7}$, and subsequent curves are plotted after varying one parameter. The PR outage for the base curve shows a gradual increase with β_r. The cut-off power level prevents transmissions to far away cognitive receivers. Thus, transmissions are limited to receivers nearby, and the probability of these increases with β_r. The curve for $M = 2$ shows a similar trend. However, the PR outage is slightly less because a cognitive transmitter only has the opportunity to connect to a maximum of 2 receivers. The curves when λ_r increases and P_s decreases differ significantly from the base curve. In both of these curves, the outage increases initially, and subsequently decreases. When P_s is lower and λ_r is higher, the cut-off power would have a lower effect, and transmission is possible to receivers far away. As $\beta_r \to 1$, transmissions occur mainly to close-by receivers, and the PR outage drops. It is interesting to note that when $M = 10$, a lower P_s and a higher λ_r result in an increased outage.

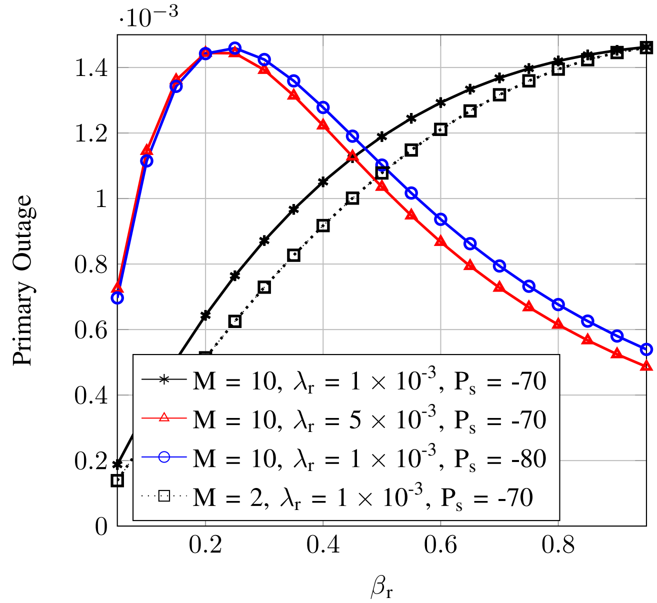

Fig. 7: Scheme 3: Primary receiver outage probability vs the availability of a cognitive receiver β_r for different M, λ_r, and P_s (dBm). $P_c = -30$ dBm, $\alpha = 3$, and $\lambda_t = 0.001$.

The PR outage is plotted vs the cognitive transmitter cut-off power level P_c for Scheme 3 in Fig. 8. The curves show an initial increase in outage before saturation. This occurs because the required transmit power is lower than P_c most of the time. Thus, any further increase in P_c would have negligible effect. When the number of receivers a cognitive transmitter attempts to connect (M) increases, the PR outage increases because the probability of associating with a receiver increases for each cognitive transmitter. However the amount of the increase decreases with M. For low P_c, M has almost no affect because transmissions to far away receivers is difficult.

D. Iterative scheme

Fig. 9 plots the probability that a cognitive transmitter is cut-off vs the target outage probability of the PR ($P_{OUT,max}$) while varying the cognitive transmitter receiver densities for the iterative scheme. From this figure, it is possible to get an insight on the required densities of the cognitive transmitters and receivers to achieve a given performance target. If very low PR outages are required (below -40dBm), it is not possible to use the given densities meaningfully. In other words, the cognitive transmitters would be cut-off most of the time they need to transmit. Intuitively, for a target $P_{OUT,max}$, the best cognitive transmitter performance is achieved when the cognitive transmitter density (λ_t) is low, and the cognitive receiver density λ_r is high. It should also be noted that increasing λ_r provides better cognitive performance than decreasing λ_t.

VI. Conclusion

This paper has investigated the aggregate I from a random network of cognitive nodes which are modeled as spatially distributed independent PPPs. Multiple power control,

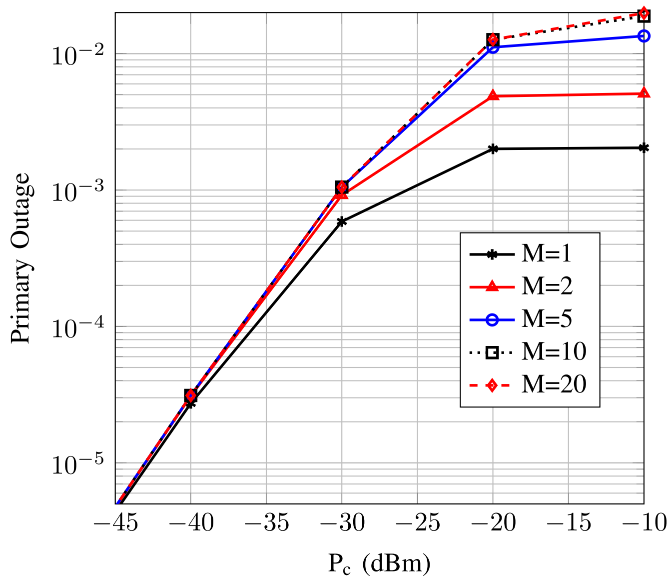

Fig. 8: Scheme 3: Primary receiver outage probability vs the cut-off power level P_c for different M. $\alpha = 3$, $\lambda_t = 0.001$, $\lambda_r = 0.001$, and $P_s = -70$ dBm.

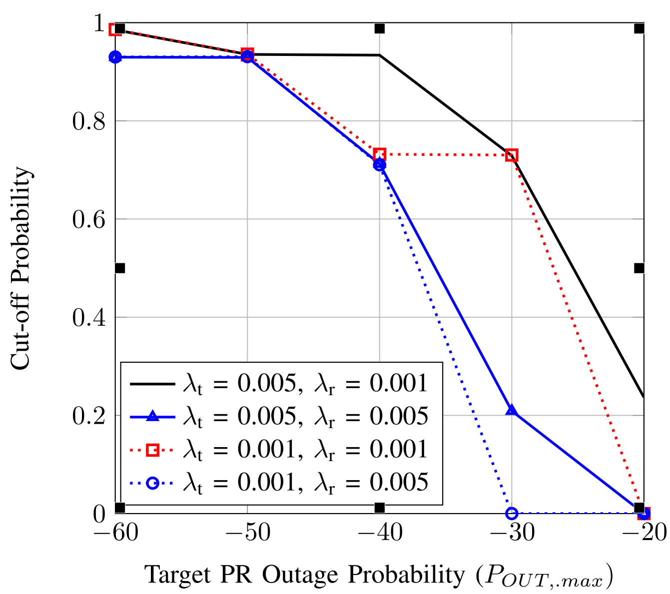

Fig. 9: Iterative Scheme: The probability that a cognitive transmitter is cut-off from transmission vs the target outage probability of the PR ($P_{OUT,max}$). $\alpha = 3$, $P_p = -10$ dBm, and $P_s = -80$ dBm.

contention control, and receiver association schemes were proposed. The MGF and mean of the aggregate I of each scheme, and the PR outage probability were derived. This study provides the following main insights. First, we find that the cognitive transmission/receiver thresholds and the receiver density significantly impact the primary performance. Second, there is a trade-off in the primary and cognitive network performances. Third, having CSI information provides marginally better primary system performance while having a slightly poorer performance with respect to the cognitive transmitter cut-off probability. Fourth, feedback information from the primary system enables a higher cognitive system availability while guaranteeing a fixed primary performance. Future research directions include considering random motion of cognitive nodes, having multiple primary receivers, and estimating the cognitive network capacity.

Appendix I :Proof of $M_{I_i}(s)$ for Scheme 5

Similar to Scheme 2, the interference from $\phi_{t,i}$ (4) is written as $I_i = B_i P_i |h_i|^2 r_i^{-\alpha}$. The parameter B_i is defined similar to Q_i as $B_i = \text{Bernoulli}(b_i)$, where $b_i = \Pr[P_i < P_c]$.

Any given transmitter sees receivers distributed as a homogeneous PPP with intensity λ_r in $\mathbb{R}^2$ with it at the center. We first show that the received power of a homogeneous PPP with intensity λ_r, path loss exponent α and Rayleigh fading is equivalent to that generated by a non-homogeneous PPP with a path loss exponent of 1 and no fading having an intensity of $\lambda_{r,3}$ (see Appendix III) where

$$\lambda_{r,3}(r) = \frac{2\pi}{\alpha}\lambda_r r^{\frac{2}{\alpha}-1}\Gamma(\frac{2}{\alpha}+1), 0 < r < \infty. \tag{33}$$

Now, under this new PPP, the effects of the path loss exponent and fading have been normalized. The neighbor with the lowest distance metric of the new PPP (note that this metric is not the distance in its true sense) would be the receiver having the highest received power. Thus, the CDF of the distance to the receiver having the highest received power can easily be found using the void probability. Let r_p be the distance from a transmitter to the receiver having the highest received power. Then,

$$F_{r_p}(x) = 1 - \Pr[\text{zero nodes in a line segment of length } x].$$

Using (1), $F_r(x)$ is found as

$$F_{r_p}(x) = 1 - e^{-\int_0^x \lambda_{r,3} dr} = 1 - e^{-\pi\lambda_r\Gamma(\frac{2}{\alpha}+1)x^{\frac{2}{\alpha}}}, 0 < x < \infty. \tag{34}$$

The PDF of this distribution f_{r_p} becomes

$$f_{r_p}(x) = \frac{2\pi}{\alpha}\lambda_r\Gamma(\frac{2}{\alpha}+1)x^{\frac{2}{\alpha}-1}e^{-\pi\lambda_r\Gamma(\frac{2}{\alpha}+1)x^{\frac{2}{\alpha}}}, 0 < x < \infty. \tag{35}$$

Now, we return to our original objective of deriving the MGF of the interference from $\phi_{t,i}$ ($M_{I_i}(s)$). In order to ensure a constant receiver power of P_s, the transmitter transmits at a power of $P_s r_p$ (note that the path loss and fading are not present in the equation, but rather is included within r_p). Then,

$$b_i = \Pr[P_s r_p < P_c] = 1 - e^{-\pi\lambda_r\Gamma(\frac{2}{\alpha}+1)(\frac{P_c}{P_s})^{\frac{2}{\alpha}}}.$$

We now write $M_{I_i}(s)$ as

$$M_{I_i}(s) = 1 - b_i + \frac{\pi}{A_t}\int_0^{(\frac{P_c}{P_s})}\left((\mathcal{U}(R_g)-1)R_g^2 - (\mathcal{U}(R_e)-1)R_e^2\right) \times f_{r_p}(r_p)dr_p, \tag{36}$$

where $\mathcal{U}(x) = {}_2F_1\left(1, \frac{2}{\alpha}; 1+\frac{2}{\alpha}, -\frac{x^\alpha}{sP_s r_p}\right)$. A closed-form equation for $M_{I_i}(s)$ is obtained as

$$M_{I_i}(s) = e^{-\pi\lambda_r\Gamma(\frac{2}{\alpha}+1)(\frac{P_c}{P_s})^{\frac{2}{\alpha}}} + \frac{2\pi}{A_t}\sum_{t=0}^{\infty}\left(\frac{-sP_s}{(\pi\lambda_r\Gamma(\frac{2}{\alpha}+1))^{\frac{\alpha}{2}}}\right)^t \times\left(\frac{R_e^{2-\alpha t}-R_g^{2-\alpha t}}{2-\alpha t}\right)\left(\Gamma\left(\frac{\alpha t}{2}+1\right)\right. \left.-\Gamma\left(\frac{\alpha t}{2}+1, \pi\lambda_r\Gamma(\frac{2}{\alpha}+1)\left(\frac{P_c}{P_s}\right)^{\frac{2}{\alpha}}\right)\right), \alpha > 2. \quad (37)$$

Appendix II :Proof of the mapping procedure

The intensity function of a PPP in $\mathbb{R}^2$ can be transformed from (x, y) coordinates to polar coordinates (r, θ) by using the Mapping theorem [36] (This is used to convert the 2-D PPP to a 1-D PPP) For a homogeneous PPP of intensity λ, the intensity function in polar coordinates is given by

$$\lambda^*(r, \theta) = \lambda\ r, \quad 0 < r < \infty, 0 < \theta < 2\pi. \quad (38)$$

The received power from an interfering node does not depends on its angular position but on its distance to the receiver. Therefore, the PPP on $\mathbb{R}^2$ is mapped onto the positive real axis while preserving the distance distribution. Using the Mapping theorem, it can be shown that the mapped points on the positive real axis form a PPP. The intensity of the this PPP $\lambda_{r,1}(r)$ can be obtained by integrating out θ [36]. Therefore,

$$\lambda_{r,1}(r) = \int_0^{2\pi} \lambda\ r d\theta = 2\pi\lambda r, \quad 0 < r < \infty. \quad (39)$$

The received power at a receiver from a cognitive transmitter is given by $P_i r_p^{-\alpha}|h_i|^2$. In the following step, we use the Mapping theorem to obtain a new PPP which generates a received power identical to what is generated by the above PPP with intensity $\lambda_{r,1}$, but with a path loss exponent of 1. The intensity function of the new PPP $\lambda_{r,2}(r)$ can be derived as follows: Consider the mapping function $f(r) = r^\alpha$. In the mapping process, points in the line segment $(r, r+\Delta r)$ in the new PPP are from the $(r^{-\alpha}, (r+\Delta r)^{-\alpha})$ line segment of the PPP with intensity $\lambda_{r,1}(r)$. The number of points in the line segment $(r, r+\Delta r)$ of the new PPP can be written as [49]

$$N[r, r+\Delta r] = \int_{r^{-\alpha}}^{(r+\Delta r)^{-\alpha}} \lambda_{r,1}(r) dr. \quad (40)$$

Using the change of variable $t = r^\alpha$,

$$N[r, r+\Delta r] = \int_r^{r+\Delta r} \lambda_{r,1}\left(\frac{1}{t}\right)\frac{t^{\frac{1}{\alpha}-1}}{\alpha} dt. \quad (41)$$

Therefore, according to the Mapping theorem [36] the intensity of the new PPP is given by [49]

$$\lambda_{r,2}(r) = \lambda_{r,1}\left(\frac{1}{r}\right)\frac{r^{\frac{1}{\alpha}-1}}{\alpha}, \quad 0 < r < \infty$$
$$= \frac{2\pi\lambda_r r^{\frac{2}{\alpha}-1}}{\alpha}, \quad 0 < r < \infty. \quad (42)$$

In the following step, we use the product space representation, the Marking theorem [36, Sec. 5.2], and the Mapping theorem to obtain a new PPP which generates the identical received power, but with a path loss exponent of 1 and no fading. The intensity function of the new PPP $\lambda_{r,3}(r)$ can be derived as [49]

$$\lambda_{r,3}(r) = E_{|h|^2}\left[|h|^2\lambda_{r,2}(r|h|^2)\right], \quad 0 < r < \infty. \quad (43)$$

For Rayleigh fading channels (43) can be written as

$$\lambda_{r,3}(r) = \frac{2\pi}{\alpha}\lambda_r r^{\frac{2}{\alpha}-1} E_{|h_i|^2}[(|h_i|^2)^{\frac{2}{\alpha}}], 0 < r < \infty.$$
$$= \frac{2\pi}{\alpha}\lambda_r r^{\frac{2}{\alpha}-1}\Gamma\left(\frac{2}{\alpha}+1\right), 0 < r < \infty. \quad (44)$$

Note that the limits of r do not change because the cognitive receivers are distributed in a 2-D field. This would not be the case otherwise.

References

[1] S. Kusaladharma, P. Herath, and C. Tellambura, "Impact of transmit power control on aggregate interference in underlay cognitive radio networks," in *Proc. IEEE ICC*, June 2014, pp. 1–6.

[2] A. Goldsmith, S. Jafar, I. Maric, and S. Srinivasa, "Breaking spectrum gridlock with cognitive radios: An information theoretic perspective," *Proc. IEEE*, vol. 97, no. 5, pp. 894–914, 2009.

[3] K. Arshad, R. Mackenzie, U. Celentano, A. Drozdy, S. Leveil, G. Mange, J. Rico, A. Medela, and C. Rosik, "Resource management for qos support in cognitive radio networks," *IEEE Commun. Mag.*, vol. 52, no. 3, pp. 114–120, March 2014.

[4] X. Hong, J. Wang, C.-X. Wang, and J. Shi, "Cognitive radio in 5g: a perspective on energy-spectral efficiency trade-off," *IEEE Commun. Mag.*, vol. 52, no. 7, pp. 46–53, July 2014.

[5] S. Srinivasa and S. Jafar, "Cognitive radios for dynamic spectrum access - the throughput potential of cognitive radio: A theoretical perspective," *IEEE Commun. Mag.*, vol. 45, no. 5, pp. 73–79, May 2007.

[6] C. han Lee and M. Haenggi, "Delay analysis of spatio-temporal channel access for cognitive networks," in *Proc. IEEE ICC*, June 2011, pp. 1–5.

[7] P. Mach and Z. Becvar, "QoS-guaranteed power control mechanism based on the frame utilization for femtocells," *EURASIP Journal on Wireless Communications and Networking*, vol. 2011, 2011.

[8] A. Molisch, *Wireless Communications*. Wiley-IEEE Press, 2011.

[9] J. Jang and K.-B. Lee, "Transmit power adaptation for multiuser OFDM systems," *IEEE J. Sel. Areas Commun.*, vol. 21, no. 2, pp. 171–178, 2003.

[10] D. Qiao, S. Choi, and K. Shin, "Interference analysis and transmit power control in IEEE 802.11a/h wireless LANs," *IEEE/ACM Trans. Networking*, vol. 15, no. 5, pp. 1007–1020, 2007.

[11] S. Gong, P. Wang, Y. Liu, and W. Zhuang, "Robust power control with distribution uncertainty in cognitive radio networks," *IEEE J. Sel. Areas Commun.*, vol. 31, no. 11, pp. 2397–2408, 2013.

[12] C. Sun, Y. Alemseged, H.-N. Tran, and H. Harada, "Transmit power control for cognitive radio over a Rayleigh fading channel," *IEEE Trans. Veh. Technol.*, vol. 59, no. 4, pp. 1847–1857, 2010.

[13] Z. Chen, C.-X. Wang, X. Hong, J. Thompson, S. Vorobyov, X. Ge, H. Xiao, and F. Zhao, "Aggregate interference modeling in cognitive radio networks with power and contention control," *IEEE Trans. Commun.*, vol. 60, no. 2, pp. 456–468, Feb. 2012.

[14] Y. Qu, J. Fang, and S. Zhang, "Nearest neighbor nodes and connectivity of three-dimensional wireless sensor networks with poisson point field," in *Proc. IEEE ICCSIT*, vol. 2, July 2010, pp. 269–272.

[15] A. Rabbachin, T. Q. S. Quek, H. Shin, and M. Z. Win, "Cognitive network interference," *IEEE J. Sel. Areas Commun.*, vol. 29, no. 2, pp. 480–493, Feb. 2011.

[16] A. Busson, B. Jabbari, A. Babaei, and V. Veque, "Interference and throughput in spectrum sensing cognitive radio networks using point processes," *Communications and Networks, Journal of*, vol. 16, no. 1, pp. 67–80, Feb 2014.

[17] H. ElSawy and E. Hossain, "Two-tier hetnets with cognitive femtocells: Downlink performance modeling and analysis in a multichannel environment," *IEEE Trans. Mobile. Computing*, vol. 13, no. 3, pp. 649–663, March 2014.

[18] H. ElSawy, E. Hossain, and M. Haenggi, "Stochastic geometry for modeling, analysis, and design of multi-tier and cognitive cellular wireless networks: A survey," *Communications Surveys Tutorials, IEEE*, vol. 15, no. 3, pp. 996–1019, Third 2013.

[19] L. Vijayandran, P. Dharmawansa, T. Ekman, and C. Tellambura, "Analysis of aggregate interference and primary system performance in finite area cognitive radio networks," *IEEE Trans. Commun.*, vol. PP, no. 99, pp. 1–12, 2012.

[20] N. Lee, X. Lin, J. G. Andrews, and R. W. Heath, "Power control for d2d underlaid cellular networks: Modeling, algorithms and analysis," *CoRR*, vol. abs/1305.6161, 2013.

[21] A. Babaei and B. Jabbari, "Interference modeling and avoidance in spectrum underlay cognitive wireless networks," in *Proc. IEEE ICC*, May 2010, pp. 1–5.

[22] S. Kusaladharma and C. Tellambura, "On approximating the cognitive radio aggregate interference," *IEEE Wireless Commun. Lett.*, vol. 2, no. 1, pp. 58–61, 2013.

[23] M. J. Rahman and X. Wang, "Probabilistic analysis of mutual interference in cognitive radio communications," in *Proc. IEEE GLOBECOM*, Dec. 2011, pp. 1–5.

[24] C.-H. Lee and C.-Y. Shih, "Coverage analysis of cognitive femtocell networks," *IEEE Wireless Commun. Lett.*, vol. 3, no. 2, pp. 177–180, April 2014.

[25] S. Kusaladharma and C. Tellambura, "Aggregate interference analysis for underlay cognitive radio networks," *IEEE Wireless Commun. Lett.*, vol. 1, no. 6, pp. 641–644, 2012.

[26] M. Hanif, M. Shafi, P. Smith, and P. Dmochowski, "Interference and deployment issues for cognitive radio systems in shadowing environments," in *Proc. IEEE ICC*, Jun. 2009, pp. 1–6.

[27] X. Hong, C.-X. Wang, and J. Thompson, "Interference modeling of cognitive radio networks," in *Proc. IEEE VTC*, May 2008, pp. 1851–1855.

[28] S. Kusaladharma and C. Tellambura, "Impact of beacon misdetection on aggregate interference for hybrid underlay-interweave networks," *IEEE Wireless Commun. Lett.*, vol. 17, no. 11, pp. 2052–2055, November 2013.

[29] C.-H. Lee and M. Haenggi, "Interference and outage in poisson cognitive networks," *IEEE Trans. Wireless Commun.*, vol. 11, no. 4, pp. 1392–1401, Apr. 2012.

[30] A. Rabbachin, A. Conti, and M. Win, "Wireless network intrinsic secrecy," *IEEE Trans. Netw.*, vol. 23, no. 1, pp. 56–69, Feb 2015.

[31] X. Zhang and M. Haenggi, "Random power control in poisson networks," *IEEE Trans. Commun.*, vol. 60, no. 9, pp. 2602–2611, September 2012.

[32] G. Alfano, M. Garetto, and E. Leonardi, "New directions into the stochastic geometry analysis of dense csma networks," *IEEE Trans. Mobile Computing*, vol. 13, no. 2, pp. 324–336, Feb 2014.

[33] S. Weber, J. Andrews, and N. Jindal, "The effect of fading, channel inversion, and threshold scheduling on ad hoc networks," *IEEE Trans Info. Theory*, vol. 53, no. 11, pp. 4127–4149, Nov 2007.

[34] C. Tellambura, A. Mueller, and V. Bhargawa, "Analysis of m-ary phase-shift keying with diversity reception for land-mobile satellite channels," *IEEE Trans. Veh. Tech.*, vol. 46, no. 4, pp. 910–922, Nov 1997.

[35] Y. Dhungana and C. Tellambura, "Uniform approximations for wireless performance in fading channels," *IEEE Trans. Commun.*, vol. 61, no. 11, pp. 4768–4779, November 2013.

[36] J. F. Kingman, *Poisson Processes*. Oxford University Press, 1993.

[37] I. Gradshteyn and I. Ryzhik, *Table of integrals, Series, and Products*, 7th ed. Academic Press, 2007.

[38] P. C. Pinto and M. Z. Win, "Communication in a Poisson field of interferers–part I: Interference distribution and error probability," *IEEE Trans. Wireless Commun.*, vol. 9, no. 7, pp. 2176–2186, Jul. 2010.

[39] E. Salbaroli and A. Zanella, "Interference analysis in a Poisson field of nodes of finite area," *IEEE Trans. Veh. Technol.*, vol. 58, no. 4, pp. 1776–1783, May 2009.

[40] A. Baddeley, I. Barany, R. Schneider, and W. Weil, *Spatial Point Processes and their Applications*. Springer, 2007.

[41] D. Moltchanov, "Distance distributions in random networks," *Ad Hoc Networks*, vol. 10, no. 6, pp. 1146–1166, 2012. [Online]. Available: http://www.sciencedirect.com/science/article/pii/S1570870512000224

[42] D. Stoyan, W. S. Stoyan, Kendall, and J. Mecke, *Stochastic Geometry and it's Applications*. John Wiley & Sons Ltd., 1995.

[43] J. Andrews, F. Baccelli, and R. Ganti, "A tractable approach to coverage and rate in cellular networks," *IEEE Trans. Commun.*, vol. 59, no. 11, pp. 3122–3134, 2011.

[44] A. Goldsmith, *Wireless Communications*. Cambridge University Press, 2005.

[45] Q. Cui, Y. Zhang, and X. Tao, "Hybrid-pilot based downlink CSI feedback scheme with zero-overhead," in *Proc. IEEE VTC*, Sept 2009, pp. 1–4.

[46] S.-R. Cho and W. Choi, "Coverage and load balancing in heterogeneous cellular networks with minimum cell separation," *IEEE Trans. Mobile Computing*, vol. 13, no. 9, pp. 1955–1966, Sept 2014.

[47] M. Haenggi, "Mean interference in hard-core wireless networks," *IEEE Commun. Lett.*, vol. 15, no. 8, pp. 792–794, August 2011.

[48] S. Kusaladharma, P. Herath, and C. Tellambura, "Impact of transmit power control and receiver association on interweave network interference," in *Proc. IEEE VTC*, Sept 2014, pp. 1–5.

[49] P. Madhusudhanan, J. Restrepo, Y. Liu, T. Brown, and K. Baker, "Downlink performance analysis for a generalized shotgun cellular system," *IEEE Trans. Wireless Commun.*, vol. 13, no. 12, pp. 6684–6696, Dec 2014.

Sachitha Kusaladharma received the B.Sc. degree in electrical and telecommunication engineering (with first-class honors) from the University of Moratuwa, Sri Lanka, in 2010 and the M.Sc. degree in wireless communications from the University of Alberta, AB, Canada, in 2013. He is currently working towards the Ph.D. degree at the Department of Electrical and Computer Engineering, University of Alberta. His research interests include cognitive radio networks, communication theory, MIMO systems, wireless sensor networks.

Prasanna Herath (S'09) received the B.Sc. degree in electrical and electronics engineering (with first-class honors) from the University of Peradeniya, Sri Lanka, in 2007 and the M.Eng. degree in telecommunications from the University of Western Sydney, Australia, in 2011. He is currently working towards the Ph.D. degree at the Department of Electrical and Computer Engineering, University of Alberta, Canada.

Since 2012, he has been with Telecommunications Research Laboratories (TRTech), Edmonton, Canada. His research interests include modeling and interference mitigation in heterogeneous cellular networks, device-to-device communications, and performance analysis of communication systems.

Chintha Tellambura (F'11) received the B.Sc. degree (with first-class honor) from the University of Moratuwa, Sri Lanka, in 1986, the M.Sc. degree in Electronics from the University of London, United Kingdom, in 1988, and the Ph.D. degree in Electrical Engineering from the University of Victoria, Canada, in 1993.

He was a Postdoctoral Research Fellow with the University of Victoria (1993-1994) and the University of Bradford (1995-1996). He was with Monash University, Australia, from 1997 to 2002. Presently, he is a Professor with the Department of Electrical and Computer Engineering, University of Alberta. His current research interests include the design, modelling and analysis of cognitive radio networks, heterogeneous cellular networks and multiple-antenna wireless networks.

Prof. Tellambura served as an editor for both IEEE Transactions on Communications and IEEE Transactions on Wireless Communications and was the Area Editor for Wireless Communications Systems and Theory in the IEEE Transactions on Wireless Communications during 2007-2012. Prof. Tellambura and co-authors received the Communication Theory Symposium best paper award in the 2012 IEEE International Conference on Communications, Ottawa, Canada. He is the winner of the prestigious McCalla Professorship and the Killam Annual Professorship from the University of Alberta. Prof. Tellambura has authored or coauthored over 480 journal and conference publications with total citations more than 10,000 and an h-index of 53 (Google Scholar).